Heliyon 10 (2024) e40705

Contents lists available at ScienceDirect

Heliyon

journal homepage: www.cell.com/heliyon

Research article

Synthesis of ultra-large diameter graphene oxide flakes from natural flake graphite

Xiaohu Wang [a,1], Xin Li [b,1], Ao Li [a], Yujie Han [a], Jie Chen [b], Dongxia Huo [b], Xin Gao [b], Chunguang Wei [a,**], Zeyu Guo [c], Jun Liu [a], Junhui Dong [a,***], Ding Nan [b,*]

[a] Inner Mongolia Key Laboratory of New Materials and Surface Engineering, School of Materials Science and Engineering, School of New Energy, Inner Mongolia University of Technology, Hohhot, 010051, China
[b] College of Chemistry and Chemical Engineering, Inner Mongolia University, Hohhot, 010021, China
[c] Inner Mongolia Key Laboratory of Sandy Shrubs Fibrosis and Energy Development and Utilization, College of Materials Science and Art Design, Inner Mongolia Agricultural University, Hohhot, 010018, China

ARTICLE INFO

Keywords:
Graphene oxide
Ultra-large diameter
Interpolation method
Chemical reduction

ABSTRACT

Graphene and its derivatives are widely used in various fields due to their unique two-dimensional lamellar structure. This study aims to synthesize ultra-large graphene oxide (GO) sheets from natural flake graphite and investigate the factors influencing their size. Using a two-intercalation method based on the modified Hummers' method, we address the challenge of intercalating large-diameter graphene oxide by employing a secondary intercalation technique. Three different approaches were explored to control the size of the produced GO sheets. The results revealed that the completeness of the expansion graphite structure after initial intercalation significantly influenced the final GO sheet size, with more complete expansion leading to larger sheets. Optimal processing conditions were identified, involving soaking natural flake graphite in a mixed solution (H_2SO_4:H_2O_2 = 4:1), followed by drying at 60 °C for 24 h. Under these conditions, ultra-large GO sheets were predominantly monolayer with an average size of 220.99 μm and a maximum size of 438 μm. These monolayer GO sheets can be chemically reduced to graphene, making them promising for applications in transparent conductive films, optoelectronic devices, and aligned graphene composites.

1. Introduction

Graphene, characterized by its single-atom-thick two-dimensional lattice of carbon atoms, has garnered considerable attention in recent years due to its vast potential across diverse domains, including electronics [1,2], composites [3], sensors [4], and energy-related systems [5]. This interest stems from graphene's remarkable electrical [6–8], optical [9,10], mechanical [11–13], and thermal properties [14,15]. However, the performance of graphene is intricately linked to its preparation process. Addressing the challenge of producing high-quality graphene with these distinctive characteristics is imperative. Indeed, there exists a variety of

* Corresponding author.
** Corresponding author.
*** Corresponding author.
E-mail addresses: wcg@imut.edu.cn (C. Wei), jhdong@imut.edu.cn (J. Dong), nd@imu.edu.cn (D. Nan).
[1] These authors contributed equally to this work.

https://doi.org/10.1016/j.heliyon.2024.e40705
Received 4 October 2024; Received in revised form 22 November 2024; Accepted 25 November 2024
Available online 27 November 2024

methods for preparing graphene, including the solution-phase method [16], micromechanical exfoliation method [17], mechanical peeling with a scotch tape method [18], chemical vapor deposition method [19], and epitaxial growth method [20]. The pervasive utilization of graphene necessitates the advancement of methodologies for the economical large-scale production of graphene of exceptional quality. Aside from the solution-phase technique, alternative methods fail to exemplify the utmost efficacy in addressing the requisites of large-scale graphene applications.

The solution-phase approach, stemming from the Hummers' method, has found widespread utilization in generating graphene oxide (GO) sheets, which serve as pivotal precursors for synthesizing graphene [21]. The lateral dimensions of graphene sheets, derived from the restoration of GO, wield considerable influence over the characteristics of graphene-based electrodes and composites. The electrical conductivity of graphene aggregates is intricately influenced by the contact resistance prevailing between the graphene sheets. Larger graphene sheets, encompassing a greater unit area, possess the capacity to diminish the frequency of graphene-graphene contacts, thereby mitigating the cumulative impact of contact resistance and augmenting conductivity levels. Greater sheet dimensions exhibit enhanced efficacy in load transmission, particularly when graphene functions as a reinforcing filler within composites. Hence, the dimensions of GO directly dictate its ability to manifest the optimal advantages within applications. GO epitomizes a singular, two-dimensional structural material, encompassing individual sheets [2,22]. Characterized as a stratified substance, GO consists of hydrophilic graphene sheets embellished with oxygen functional groups, namely carboxyl, hydroxyl, or epoxy moieties, dispersed along both their basal planes and edges [23,24]. Chemical methodologies have gained extensive traction in the production of GO, yielding sheets typically characterized by diminutive lateral dimensions, typically ranging from hundreds of nanometers to a few micrometers [25–28].

The original Hummers' method and its various modified iterations entail a process of oxidation followed by rigorous ultrasonication or extended mechanical agitation of the GO solution to achieve the exfoliation of GO sheets. Indeed, these methodologies often necessitate the liberal application of oxidants and intensive ultrasonication, which can lead to pronounced damage and fragmentation of the GO sheets [25]. Previous research has succeeded in enlarging the dimensions of GO sheets to a certain degree, including the control of the electric current and reduction time of an electrochemical method [29], the alteration of oxidation and exfoliation processes in a chemical method [30,31], the adjustment of the pH value of GO dispersion and realizing selective sedimentation process [32], the size fractionation by a series of centrifugation at gradually decreasing speeds [33,34], the use of stationary oxidation-monolithic crystalline swelling strategy convert graphite to ultra-large GO (e.g. the average size of 108 μm and the largest size of 256 μm) [35], the use of large natural flake graphite and pre-oxidation of natural flake graphite powders [36], and the modification of oxidation path and mechanical energy, such as shaking and sonication [37]. Zhou et al. [38] by modifying the solid-state method, single-layer GO and graphene sheets with a lateral size of up to 200 mm were successfully prepared. The large GO sheets can be completely preserved to a large extent by using gentle shaking in the stratification step. Uniform colloidal suspensions with high graphene content can be obtained by using nonionic polymer surfactants as stabilizers. These modifications make the liquid phase method more repeatable and scalable, especially for the preparation of large-size sheets. Rizwan Ur Rehman Sagar et al. [39] said that the chemical preparation methods used to prepare GO cannot produce sizes larger than microns, because these methods use a wet chemical strategy, which is not useful for the production of centimeter-scale graphene oxide. They used a SiO_2 layer (100–500 nm) as a catalyst and oxygen donor for the production of large-area GO by chemical vapor deposition using industrial production methods. Despite efforts to optimize the synthesis process, only limited success has been achieved in breaking the size limitation barrier (10000 μm^2) when using ultralong nano graphite as the raw material. This suggests that further research and refinement of the synthesis methodology may be necessary to overcome this limitation [40].

In our study, we explored a novel approach capable of producing uniformly high-quality, large-size monolayer GO sheets. To address the challenge of intercalating large-diameter GO (~500 μm), we opted for a secondary intercalation method. This method involves the pre-expansion of natural graphite flakes. Subsequently, the temperature and duration of subsequent intercalation were investigated. It was observed that GO produced through gradual expansion at ambient temperature maintains the original, intact lamellar structure of flake graphite to the highest degree. Through this methodology, we achieved the production of single-layer GO sheets, with dimensions of up to 438 μm in the largest size and 220.99 μm in average size.

2. Experimental

2.1. Materials

Natural flake graphite (carbon content 99.9 %, the lateral dimensions are greater than 1 mm) was supplied by natural graphite mine in Bayannur, Inner Mongolia, China. Potassium permanganate (99 %), concentrated sulfuric acid (98 %), concentrated phosphoric acid (85 %), and hydrogen peroxide (30 %) were purchased from the Sinopharm Chemical Reagent Co., Ltd. All reagents can be used as received without further purification.

2.2. Preparation of expanded graphite

The effects of three different expansion processes on the expansion of natural flake graphite were investigated. The methods involved high temperature rapid expansion, high temperature slow expansion, and room temperature slow expansion, each incorporating a unique intercalation and expansion process as described below.

a. High Temperature Rapid Expansion Method:

Natural flake graphite was first oxidized by potassium permanganate in concentrated sulfuric acid at 60 °C for 2 h, using a ratio of H_2SO_4 to graphite of 4:1 (w/w). The mixture was stirred continuously during the oxidation process. After 2 h, the resultant graphite intercalation compound (GIC) was filtered, washed with deionized water, and dried in an oven at 60 °C for 24 h. The dried GIC was then rapidly expanded by placing it into a muffle furnace preheated to 1000 °C, where the material was held for 1 min, resulting in the formation of expanded graphite. The expansion process was carefully monitored to ensure that the temperature was uniform and that the heating rate was consistent.

b. High Temperature Slow Expansion Method:

The high temperature slow expansion method followed a similar initial oxidation procedure to the rapid expansion method. The natural flake graphite was oxidized by $KMnO_4$ in H_2SO_4 at 60 °C for 2 h (graphite to H_2SO_4 ratio of 4:1). After the oxidation process, the resultant GIC was filtered, washed, and dried as described previously. The dried GIC was then subjected to a slow thermal expansion process. The material was placed in a furnace and heated from room temperature to 1000 °C over the course of 1 h, with a temperature ramp rate of 20 °C/min. The expansion was allowed to occur gradually under controlled heating conditions. After reaching 1000 °C, the material was held at that temperature for 5 min to complete the expansion process.

c. Room Temperature Slow Expansion Method:

In this method, natural flake graphite was intercalated using hydrogen peroxide (H_2O_2, 30 %, Sinopharm) in concentrated H_2SO_4 at 20 °C. The ratio of H_2SO_4 to H_2O_2 was maintained at 4:1 (v/v), and the mixture was stirred for 1.5 h. After intercalation, the resulting GIC was filtered and washed with deionized water until the filtrate was neutral. The material was then dried in a blast drying oven at 60 °C for 24 h. The slow expansion process occurred at room temperature, where the expanded graphite was left to desiccate in the drying oven under continuous air flow for 24 h, promoting the exfoliation and expansion of the graphite sheets. No additional high temperature heating was applied in this method.

A flowchart summarizing the three expansion methods and the corresponding material and processing parameters is shown in Fig. 1. The critical parameters for reproducibility include the exact ratios of chemicals, the oxidation times and temperatures, the precise heating rates, and the holding times during expansion, which were all carefully controlled and monitored in each method to ensure consistency across experimental runs.

2.3. Preparation of ultra-large GO sheets

Chemically-derived GO sheets are directly synthesized from ordinary natural graphite flakes using the redox method [31,33,35]. In contrast to conventional graphite, the diffusion pathways for both intercalants and oxidants are significantly protracted when natural flake graphite is used for the direct synthesis of GO [41]. This increased diffusion resistance makes it challenging to achieve the exfoliation of GO into monolayers via a single intercalation-oxidation process. As a result, the production of ultra-large GO requires the implementation of a two-step intercalation-oxidation procedure. In the first stage of this secondary process, the interlayer spacing of the graphite is expanded, and the cohesive forces between the graphite layers are reduced. In the subsequent stage, both the

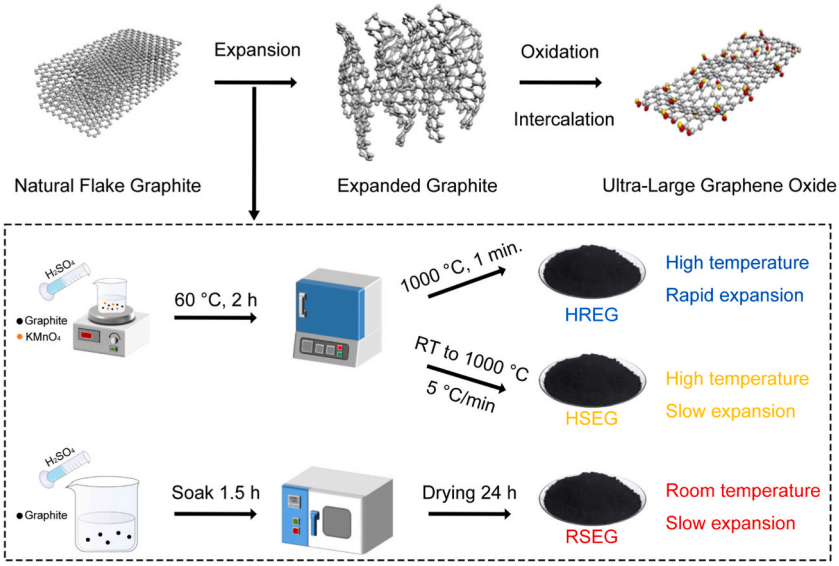

Fig. 1. The process diagram of preparing GO from natural flake graphite.

intercalating and oxidizing agents penetrate deeply into the graphite structure, resulting in complete oxidation and exfoliation of the graphite layers into GO sheets. These findings directly address the research question of how to efficiently produce large-scale graphene oxide from natural graphite flakes, suggesting that a two-step intercalation-oxidation process is necessary to overcome the diffusion challenges and achieve effective exfoliation.

2.4. Characterizations

The GO sheets prepared previously were deposited onto a Si substrate by applying a low-concentration GO dispersion (0.03 mg/L). This allowed for the examination of their structures and morphologies under a scanning electron microscope (SEM, Hitachi S-3400, Japan). A tapping-mode atomic force microscope (AFM, Bruker MultiMode 8, Germany) was employed to characterize the thickness of the layered structure of GO sheets. The structures of expanded graphite were investigated by X-ray diffraction (XRD, Rigaku D/Max-2500/PC, Japan) using Cu Kα radiation at a scanning rate of 2°/min over the 2θ range of 20°–50°. The surface chemistries of GO were characterized using a Fourier transform infrared spectroscope (FTIR, Bruker Tensor II, Germany), and functional groups were further confirmed by the FITR spectroscopy. The structure of GO sheets was assessed using a Micro-Raman spectrometer (iHR320, Jobin Yvon Technology, Japan) with laser excitation at a wavelength of 532 nm.

3. Results and discussion

3.1. Characterization of expanded graphite

Expanded graphite that underwent high temperature rapid expansion, high temperature slow expansion, and room temperature slow expansion methods were denoted as HREG, HSEG, and RSEG, respectively. And the SEM images were presented in Fig. 2.

The HREG obtained through the high temperature rapid expansion method distinctly exhibits fragmentation (Fig. 2a). In contrast, the HSEG synthesized via high temperature slow expansion method demonstrates the capability to preserve a robust graphite sheet structure (Fig. 2b). The RSEG derived from room temperature slow expansion method maintains a intact sheet-like structure, as depicted in Fig. 2c, in contrast to those produced via the first two methods. Notably, RSEG exhibits only channels formed by gas overflow between layers, with no apparent signs of graphite fragmentation. The rapid heating of expanded graphite facilitates the rapid decomposition of H_2SO_4 molecules between the graphite layers and the swift oxidation of oxygen-containing functional groups, yielding gas. This subsequent gas overflow from the graphite layers exerts a potent impact, ultimately leading to the fracture of the graphite layers. In order to investigate the impact of various expansion processes on the crystal interlayer structure of expanded graphite, XRD analysis was conducted, and patterns are presented in Fig. 3.

Based on the characteristic peak of graphite (022) and utilizing the Bragg equation $\lambda = 2d\sin\theta$ (where d represents the interlayer spacing, λ is the X-ray wavelength, and θ is the grazing angle). In comparison, the interlayer spacing of HREG, HSEG, and RSEG is measured at 0.336 nm, 0.337 nm, and 0.338 nm, respectively. HREG expansion entails the instantaneous expansion of expandable graphite at high temperatures, resulting in a larger interlayer spacing. HSEG expansion involves the gradual heating of expandable graphite from room temperature to 1000 °C, allowing for the slow overflow of gas from the graphite layers as the decomposition of H_2SO_4 molecules and the reduction of oxygen-containing functional groups occur. This leads to a slight increase in the spacing between the graphite layers. RSEG utilizes sulfuric acid molecules to facilitate the diffusion of hydrogen peroxide into the graphite interlayer. Simultaneously, hydrogen peroxide undergoes self-decomposition at room temperature, with the resulting oxygen molecules gradually overflowing from the graphite interlayer, thereby expanding the interlayer spacing of the graphite.

3.2. Characterization of GO

The primary disparity among the three methodologies resides in the manner in which the natural graphite flakes are expanded into expanded graphite. The structural integrity of the expanded graphite sheet conspicuously impacts the size distributions of GO. SEM images depicting the GO sheets, accompanied by their respective size distributions, are presented in Fig. 4. An overwhelming majority of the GO sheets exhibited excellent dispersion in the form of monolayers. Consequently, the expanded graphite generated through these three methodologies can be readily and comprehensively stripped down to a solitary layer of GO.

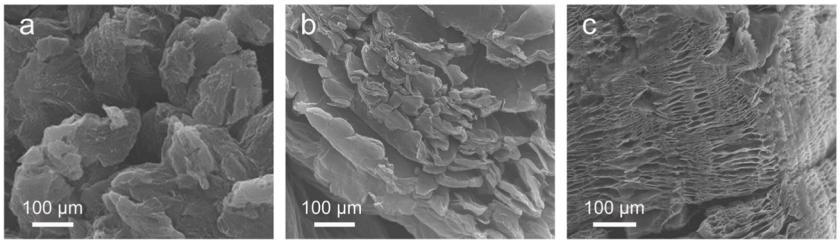

Fig. 2. SEM images of expanded graphite that underwent high temperature rapid expansion method (a), high temperature slow expansion method (b), and room temperature slow expansion method RSEG (c).

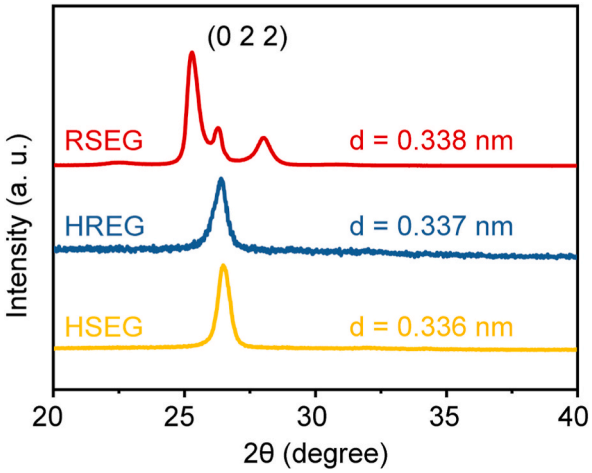

Fig. 3. XRD patterns of HREG, HSEG, and RSEG.

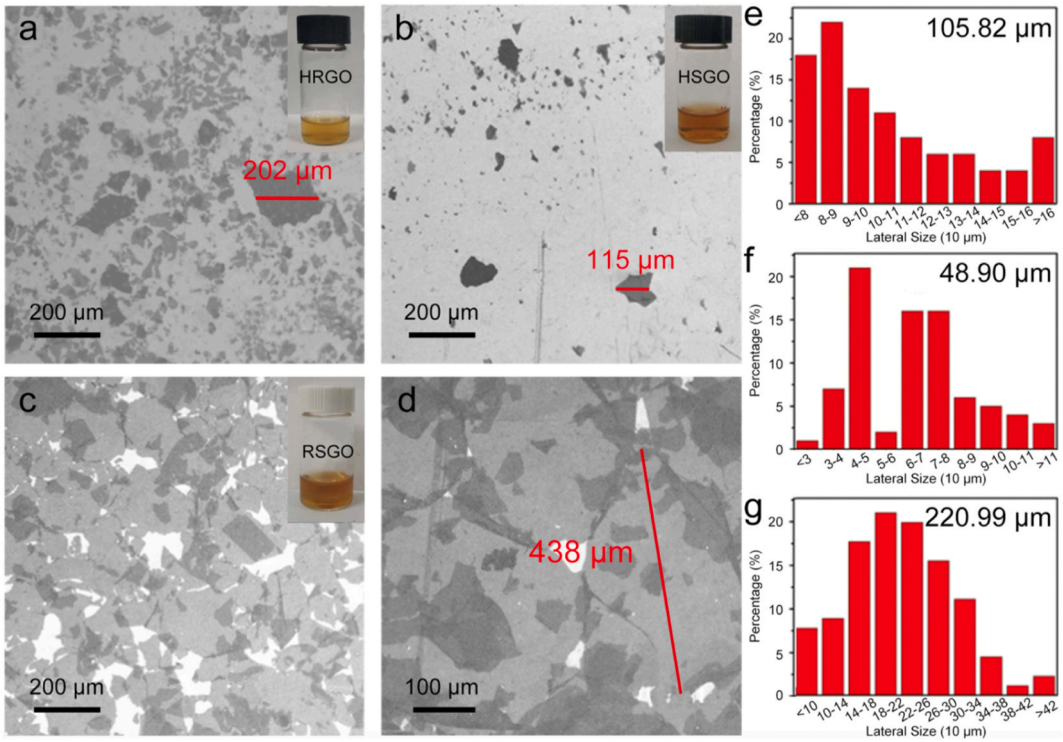

Fig. 4. SEM images of HRGO (a), HSGO (b), RSGO (c), and magnification diagram of RSGO (d). (Insets, Stable dispersion of HRGO, HSGO, and RSGO) Size distribution histograms of HRGO (e), HSEG (f), and RSEG (g).

The SEM images depicted in Fig. 4 illustrate that the lateral dimensions of GO prepared via the high temperature rapid expansion method (HRGO), high temperature slow expansion method (HSGO), and room temperature slow expansion method (RSGO) methodologies approximate 202 μm (Figs. 4a), 115 μm (Figs. 4b), and 438 μm (Fig. 4c and **d**), respectively. The lateral dimensions of the GO prepared in this study surpass those reported in previous research [39] by a factor of two, signifying a notable increase in size. Research has demonstrated that GO sheets ranging from 100 to 400 μm in lateral size have the capability to yield high-performance transparent conductive films, exhibiting electrical conductivities and transparencies on par with those of the industrial standard material, ITO [33]. The size distributions of GO sheets derived from various expanded graphite samples are depicted in Fig. 4e–g. The average lateral size of HRGO measures 48.9 μm. The average lateral size of HSGO is 105.82 μm, with 46 % exceeding 100 μm. The average lateral size of RSGO is 220.99 μm, with 46 % exceeding 220 μm. Due to the swift expansion of the GIC during the expansion process, the structure of the graphite sheet becomes fragmented. Consequently, the ultra-large natural graphite loses its preparatory advantages in the

production of GO, and the resultant expanded graphite size is akin to that of GO prepared using conventional graphite. Conversely, transitioning to a mild expansion mode curtails the gas leakage rate from the graphite layer, notably preserving the integrity of the graphite sheet structure and leading to a discernible increase in the diameter of the resulting GO sheet. When the gas produced by the decomposition of the epoxy functional group is substituted with oxygen generated by the decomposition of hydrogen peroxide at room temperature, the slow decomposition rate of hydrogen peroxide allows for a controlled release of oxygen. This controlled release of oxygen ensures that it overflows from the graphite layer, providing optimal protection to the graphite sheet structure. Additionally, this process leads to an increase in the spacing between the graphite layers, further enhancing the properties of the prepared GO. Therefore, room temperature slow expansion method effectively leverages the advantages offered by natural flake graphite in the production of ultra-large GO and maximizes its potential benefits. The AFM images depicted in Fig. 5 showcase GO dispersed on mica sheets. It is worth noting that the thickness of the prepared HRGO (as shown in Fig. 5a), HSGO (as shown in Fig. 5b), and RSGO (as shown in Fig. 5c) samples is ~1.3 nm, indicating that they all possess a monolayer structure [42].

Raman and FTIR measurements, as shown in Fig. 6, further confirm the formation of GO using the three approaches. The primary analysis in the Raman spectra focuses on the intensity ratio of the D and G bands (I_D/I_G), which serves as a crucial indicator of GO formation and structural characteristics. The D-band, located around 1350 cm^{-1}, arises from the disordered structure of graphene. This band is associated with the presence of disorder in sp^2-bonded carbon systems. The resonance Raman signal corresponding to the vibrational A_{1g} mode is induced by changes in the basal plane of graphene due to oxidative processes. This disruption in the sp^2 lattice leads to the activation of the D-band, providing insight into the level of disorder and defects present within the GO structure.

The G-band, observed at approximately 1585 cm^{-1}, is attributed to the doubly degenerate phonon mode with E_{2g} symmetry. This mode corresponds to the in-plane stretching vibrations of the C−C bonds in graphitic materials. The presence and intensity of the G-band provide information about the degree of graphitization and the presence of sp^2-bonded carbon atoms in the material [43]. In the Raman spectra delineated in Fig. 6a, HRGO, HSGO and RSGO samples manifest the characteristic D-band and G-band with I_D/I_G ratios of 0.995, 1.085, and 1.013, respectively. The elevated I_D/I_G ratio observed in HSGO can be ascribed to an increased prevalence of edge defects. In the FTIR spectrum presented in Fig. 6b, all samples display characteristic −OH, −COOH, and C−O stretching vibrations, respectively. This observation signifies that all GO possess identical functional groups and exhibit comparable oxidation effects.

3.3. Discussion

Currently, the majority of natural graphite flakes serve as precursor materials for the synthesis of GO [21,44]. Nevertheless, achieving complete oxidation of graphite flakes is a protracted process. Notably, the conventional Hummers' method, by itself, typically requires merely 2 h. However, prior to the application of the Hummers' method, a duration of 6 h is typically required to circumvent incomplete oxidation of graphite-core/GO shell particles [44]. This step is crucial to ensure that the oxidation reaches a sufficiently high degree, particularly in cases where the graphite flakes are relatively large or possess uneven structural properties.

An effective strategy to enhance oxidation efficiency involves augmenting the effective surface area of the reactive graphite [45]. Natural graphite flakes, due to their relatively large and compact nature, pose a significant challenge in terms of reactivity. To overcome this, intercalation with appropriate molecules or ions—such as sulfuric acid, nitric acid, metal chlorides, and alkali metals—can significantly enhance their oxidation potential [45–48]. The intercalating agents facilitate the insertion of oxidizing species between the graphite layers, thereby increasing the number of reaction sites available for oxidation. This mechanism is crucial for enhancing the reactivity of graphite and enabling more efficient conversion to GO.

However, a challenge arises from the diffusion of intercalating agents into large natural graphite flakes. Given the dense structure and relatively low surface area of natural graphite, achieving uniform intercalation is difficult, and incomplete intercalation can hinder the oxidation process. To address this, the natural graphite flakes are often first converted into expandable graphite, a process that involves treating the graphite with a mixture of concentrated sulfuric acid and other agents. This expansion process significantly increases the surface area of the graphite, making it more accessible to subsequent oxidation treatments. The exfoliation of graphite into graphene nanoplatelets occurs more efficiently following this expansion, as the intercalated molecules or ions are more evenly distributed, thus promoting a more uniform oxidation process.

The expansion of expandable graphite can be attributed to the synergistic action of concentrated sulfuric acid and hydrogen peroxide. Sulfuric acid acts as a carrier for hydrogen peroxide, promoting its diffusion into the graphite layers. Once inside the graphite structure, hydrogen peroxide undergoes a self-decomposition reaction, which generates oxygen species. This decomposition reaction is particularly significant because it creates a controlled release of oxygen, leading to the formation of oxygen-rich groups (such as hydroxyl and epoxide groups) on the graphite surface. As the concentration of oxygen within the graphite layers increases, the internal

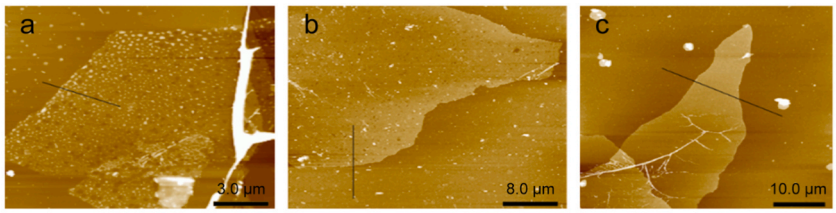

Fig. 5. AFM images of HRGO (a), HSGO (b), and RSGO (c).

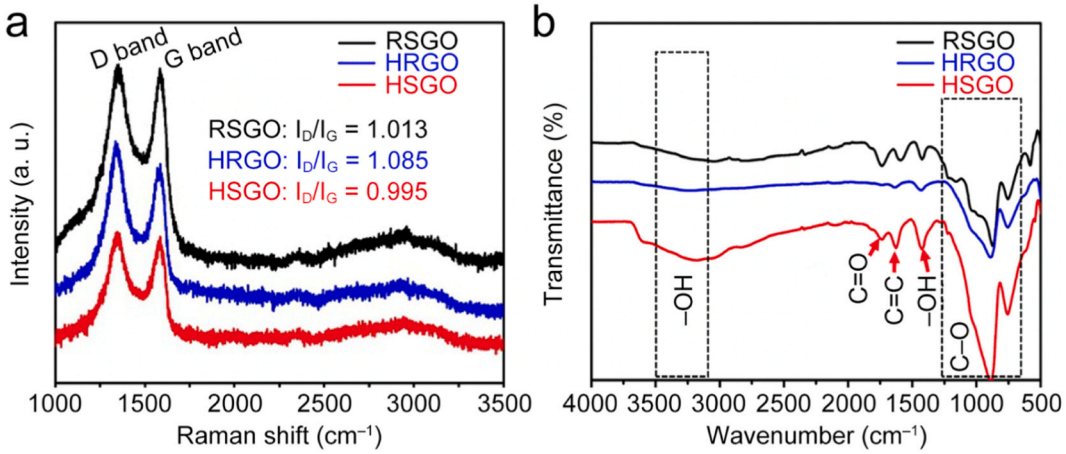

Fig. 6. Raman spectra (a) and FTIR spectra (b) of HRGO, HSGO, and RSGO.

pressure builds, causing the graphite to expand. The slow, controlled decomposition of hydrogen peroxide at ambient temperature ensures that the expansion process occurs gradually, without causing excessive disruption to the overall integrity of the graphite sheet structure. This slow expansion is essential for maintaining the structural cohesion of the graphite layers while simultaneously increasing the surface area and accessibility of the material. As a result, the expanded graphite exhibits a significantly higher reactivity towards oxidation and can be more easily converted into GO.

Furthermore, the controlled release of oxygen during the expansion process not only aids in the exfoliation of the graphite but also contributes to the formation of a more stable GO structure. The oxygenated functional groups that form during this process enhance the solubility and dispersion of GO in aqueous solutions, facilitating its use in various applications such as energy storage, catalysis, and environmental remediation. Thus, the expanded graphite serves as a crucial intermediate in the production of GO, as the pre-treatment step effectively reduces the processing time for GO synthesis and enhances the overall efficiency of the oxidation and exfoliation process.

4. Conclusion

In summary, we investigated the method of preparing ultra-large diameter GO sheets through secondary intercalation, utilizing natural flake graphite as the raw material. The primary objective of this study was to understand the impact of the graphite expansion process on the resultant diameter and properties of GO sheets. Our findings provide insight into the underlying mechanism of GO preparation from expanded graphite, specifically focusing on how different expansion methods affect the interlayer spacing and lateral size of the GO sheets. The key conclusions drawn from this research are as follows. During the expansion process, the interlayer spacings of HREG, HSEG, and RSEG were measured to be 0.336 nm, 0.337 nm, and 0.338 nm, respectively. Among these, the RSEG produced via the room temperature slow expansion method exhibited the largest interlayer spacing and demonstrated the most complete preservation of the graphite lamellar structure after expansion, compared to HREG and HSEG. Furthermore, all GO samples prepared using these three methods exhibited a consistent thickness of approximately 1.3 nm. In terms of lateral size, we found significant differences between the GO sheets derived from the three types of expanded graphite. The HRGO from HREG had an average lateral size of 48.9 μm, with a maximum size of 115 μm, while HSGO from HSEG exhibited an average lateral size of 105.82 μm, reaching a maximum of 202 μm. Notably, the RSGO obtained from the room temperature slow expansion method demonstrated an average lateral size of 220.99 μm, with an impressive maximum size of 438 μm. These results directly address the initial research question by elucidating the relationship between the graphite expansion process and the resultant GO sheet size, confirming that the slow room temperature expansion method yields the largest GO sheets with superior structural integrity. In conclusion, this work provides a novel approach for synthesizing ultra-large diameter GO materials, which holds significant implications for a range of technological applications. These findings contribute to the understanding of how to control the size and structure of GO during synthesis, which will be crucial for future developments in energy storage, environmental remediation, sensors and detection devices, and biomedical applications. Further optimization of the synthesis techniques and exploration of the material's properties will pave the way for advancing these applications.

CRediT authorship contribution statement

Xiaohu Wang: Writing – original draft, Data curation, Conceptualization. **Xin Li:** Writing – original draft, Visualization, Formal analysis, Conceptualization. **Ao Li:** Conceptualization. **Yujie Han:** Formal analysis. **Jie Chen:** Visualization. **Dongxia Huo:** Visualization. **Xin Gao:** Formal analysis. **Chunguang Wei:** Writing – review & editing, Supervision. **Zeyu Guo:** Supervision. **Jun Liu:** Supervision. **Junhui Dong:** Writing – review & editing, Supervision. **Ding Nan:** Writing – review & editing, Funding acquisition.

Data and code availability statement

Data will be made available on request.

Declaration of competing interest

The authors declare that they have no known competing financial interests or personal relationships that could have appeared to influence the work reported in this paper.

Acknowledgments

The financial supports for this work are the Inner Mongolia Major Science and Technology Project (no. 2020ZD0024), Natural Science Foundation of Inner Mongolia (No. 2024LHMS05046), Local Science and Technology Development Project of the Central Government (no. 2021ZY0006, 2022ZY0011), 2023 Inner Mongolia Autonomous Region Doctoral Research Innovation Project (no. B20231023Z), Inner Mongolia Autonomous Region key Research and Technological Achievements Transformation Plan Project (no. 2023YFHH0063), Autonomous Region higher education Carbon peak carbon neutral research project (No. STZX202206), Basic Scientific Research Expenses Program of Universities directly under Inner Mongolia Autonomous Region (No. JY20220043) and Graphite and Graphene New Materials Discipline Team of Inner Mongolia University of Technology (No. PY202066).

References

[1] H. Jang, Y.J. Park, X. Chen, T. Das, M.-S. Kim, J.-H. Ahn, Graphene-based flexible and stretchable electronics, Adv. Mater. 28 (2016) 4184–4202.
[2] J. Wu, H. Lin, D.J. Moss, K.P. Loh, B. Jia, Graphene oxide for photonics, electronics and optoelectronics, Nat. Rev. Chem 7 (2023) 162–183.
[3] J.T. Li, M.G. Stanford, W. Chen, S.E. Presutti, J.M. Tour, Laminated laser-induced graphene composites, ACS Nano 14 (2020) 7911–7919.
[4] G.M. Callicó, Image sensors go broadband, Nat. Photonics 11 (2017) 332–333.
[5] X. Li, L. Zhi, Graphene hybridization for energy storage applications, Chem. Soc. Rev. 47 (2018) 3189–3216.
[6] S. Kovalev, H.A. Hafez, K.-J. Tielrooij, J.-C. Deinert, I. Ilyakov, N. Awari, D. Alcaraz, K. Soundarapandian, D. Saleta, S. Germanskiy, M. Chen, M. Bawatna, B. Green, F.H.L. Koppens, M. Mittendorff, M. Bonn, M. Gensch, D. Turchinovich, Electrical tunability of terahertz nonlinearity in graphene, Sci. Adv. 7 (2021) eabf9809.
[7] N. Xuan, A. Xie, B. Liu, Z. Sun, Tuning electrical coupling in bilayer graphene, Carbon 201 (2023) 529–534.
[8] L. Chen, N. Li, X. Yu, S. Zhang, C. Liu, Y. Song, Z. Li, S. Han, W. Wang, P. Yang, N. Hong, S. Ali, Z. Wang, A general way to manipulate electrical conductivity of graphene, Chem. Eng. J. 462 (2023) 142139.
[9] K.L. Tsakmakidis, Stopped-light nanolasing in optical magic-angle graphene, Nat. Nanotechnol. 16 (2021) 1048–1049.
[10] G. Zanini, K. Korobchevskaya, T. Deguchi, A. Diaspro, P. Bianchini, Label-Free optical nanoscopy of single-layer graphene, ACS Nano 13 (2019) 9673–9681.
[11] Y.W. Sun, D.G. Papageorgiou, C.J. Humphreys, D.J. Dunstan, P. Puech, J.E. Proctor, C. Bousige, D. Machon, A. San-Miguel, Mechanical properties of graphene, Appl. Phys. Rev. 8 (2021) 021310.
[12] Z. Dai, G. Wang, Z. Zheng, Y. Wang, S. Zhang, X. Qi, P. Tan, L. Liu, Z. Xu, Q. Li, Z. Cheng, Z. Zhang, Mechanical responses of boron-doped monolayer graphene, Carbon 147 (2019) 594–601.
[13] A.C. McRae, G. Wei, L. Huang, S. Yigen, V. Tayari, A.R. Champagne, Mechanical control of quantum transport in graphene, Adv. Mater. 36 (2024) 2313629.
[14] F. Grote, C. Gruber, F. Börrnert, U. Kaiser, S. Eigler, Thermal disproportionation of oxo-functionalized graphene, Angew. Chem. Int. Ed. 56 (2017) 9222–9225.
[15] C. Cai, T. Wang, G. Qu, Z. Feng, High thermal conductivity of graphene and structure defects: prospects for thermal applications in graphene sheets, Chin. Chem. Lett. 32 (2021) 1293–1298.
[16] C.-J. Shih, A. Vijayaraghavan, R. Krishnan, R. Sharma, J.-H. Han, M.-H. Ham, Z. Jin, S. Lin, G.L.C. Paulus, N.F. Reuel, Q.H. Wang, D. Blankschtein, M.S. Strano, Bi- and trilayer graphene solutions, Nat. Nanotechnol. 6 (2011) 439–445.
[17] J. Zhang, X. Zhang, Z. Hou, L. Zhang, C. Li, Uniform SiOx/graphene composite materials for lithium ion battery anodes, J. Alloys Compd. 809 (2019) 151798.
[18] A. Aliprandi, M. Eredia, C. Anichini, W. Baaziz, O. Ersen, A. Ciesielski, P. Samorì, Persian waxing of graphite: towards green large-scale production of graphene, Chem. Commun. 55 (2019) 5331–5334.
[19] Z. Chen, X. Guo, L. Zhu, L. Li, Y. Liu, L. Zhao, W. Zhang, J. Chen, Y. Zhang, Y. Zhao, Direct growth of graphene on vertically standing glass by a metal-free chemical vapor deposition method, J. Mater. Sci. Technol. 34 (2018) 1919–1924.
[20] Y.-C. Han, S.-H. Yin, J.-R. Zheng, Y.-F. Hu, L. Sun, L. Zhang, Z.-Q. Tian, J. Yi, Epitaxial growth of graphene on SiC by thermal shock annealing within seconds, Adv. Funct. Mater. 34 (2024) 2307298.
[21] W.S. Hummers, R.E. Offeman, Preparation of graphitic oxide, J. Am. Chem. Soc. 80 (1958), 1339-1339.
[22] G. Eda, G. Fanchini, M. Chhowalla, Large-area ultrathin films of reduced graphene oxide as a transparent and flexible electronic material, Nat. Nanotechnol. 3 (2008) 270.
[23] D.A. Dikin, S. Stankovich, E.J. Zimney, R.D. Piner, G.H.B. Dommett, G. Evmenenko, S.T. Nguyen, R.S. Ruoff, Preparation and characterization of graphene oxide paper, Nature 448 (2007) 457–460.
[24] A.K. Geim, K.S. Novoselov, The rise of graphene, Nat. Mater. 6 (2007) 183–191.
[25] S.H. Aboutalebi, M.M. Gudarzi, Q.B. Zheng, J.-K. Kim, Spontaneous Formation of liquid crystals in ultralarge graphene oxide dispersions, Advanced Functional Mater 21 (2011) 2978–2988.
[26] X. Wang, L. Zhi, K. Müllen, Transparent, conductive graphene electrodes for dye-sensitized solar cells, Nano Lett. 8 (2008) 323–327.
[27] H.A. Becerril, J. Mao, Z. Liu, R.M. Stoltenberg, Z. Bao, Y. Chen, Evaluation of solution-processed reduced graphene oxide films as transparent conductors, ACS Nano 2 (2008) 463–470.
[28] G. Eda, Y.-Y. Lin, S. Miller, C.-W. Chen, W.-F. Su, M. Chhowalla, Transparent and conducting electrodes for organic electronics from reduced graphene oxide, Appl. Phys. Lett. 92 (2008) 233305.
[29] X.-Y. Peng, X.-X. Liu, D. Diamond, K.T. Lau, Synthesis of electrochemically-reduced graphene oxide film with controllable size and thickness and its use in supercapacitor, Carbon 49 (2011) 3488–3496.
[30] L. Zhang, J. Liang, Y. Huang, Y. Ma, Y. Wang, Y. Chen, Size-controlled synthesis of graphene oxide sheets on a large scale using chemical exfoliation, Carbon 47 (2009) 3365–3368.
[31] J. Zhao, S. Pei, W. Ren, L. Gao, H.-M. Cheng, Efficient preparation of large-area graphene oxide sheets for transparent conductive films, ACS Nano 4 (2010) 5245–5252.
[32] X. Wang, H. Bai, G. Shi, Size fractionation of graphene oxide sheets by pH-assisted selective sedimentation, J. Am. Chem. Soc. 133 (2011) 6338–6342.
[33] Q. Zheng, W.H. Ip, X. Lin, N. Yousefi, K.K. Yeung, Z. Li, J.-K. Kim, Transparent conductive films consisting of ultralarge graphene sheets produced by Langmuir–blodgett assembly, ACS Nano 5 (2011) 6039–6051.

[34] X. Lin, X. Shen, Q. Zheng, N. Yousefi, L. Ye, Y.-W. Mai, J.-K. Kim, Fabrication of highly-aligned, conductive, and strong graphene papers using ultralarge graphene oxide sheets, ACS Nano 6 (2012) 10708–10719.
[35] J. Zhang, Q. Liu, Y. Ruan, S. Lin, K. Wang, H. Lu, Monolithic crystalline swelling of graphite oxide: a bridge to ultralarge graphene oxide with high scalability, Chem. Mater. 30 (2018) 1888–1897.
[36] C.-Y. Su, Y. Xu, W. Zhang, J. Zhao, X. Tang, C.-H. Tsai, L.-J. Li, Electrical and spectroscopic characterizations of ultra-large reduced graphene oxide monolayers, Chem. Mater. 21 (2009) 5674–5680.
[37] X. Zhou, Z. Liu, A scalable, solution-phase processing route to graphene oxide and graphene ultralarge sheets, Chem. Commun. 46 (2010) 2611–2613.
[38] R.U.R. Sagar, M. Namvari, S.T. Navale, F.J. Stadler, Synthesis of scalable and tunable slightly oxidized graphene via chemical vapor deposition, J. Colloid Interface Sci. 490 (2017) 844–849.
[39] S. Pan, I.A. Aksay, Factors controlling the size of graphene oxide sheets produced via the graphite oxide route, ACS Nano 5 (2011) 4073–4083.
[40] J. Jia, C.-M. Kan, X. Lin, X. Shen, J.-K. Kim, Effects of processing and material parameters on synthesis of monolayer ultralarge graphene oxide sheets, Carbon 77 (2014) 244–254.
[41] C. Li, Y. Shi, X. Chen, D. He, L. Shen, N. Bao, Controlled synthesis of graphite oxide: formation process, oxidation kinetics, and optimized conditions, Chem. Eng. Sci. 176 (2018) 319–328.
[42] D. Li, M.B. Müller, S. Gilje, R.B. Kaner, G.G. Wallace, Processable aqueous dispersions of graphene nanosheets, Nat. Nanotechnol. 3 (2008) 101–105.
[43] L.G. Cançado, A. Jorio, E.H.M. Ferreira, F. Stavale, C.A. Achete, R.B. Capaz, M.V.O. Moutinho, A. Lombardo, T.S. Kulmala, A.C. Ferrari, Quantifying defects in graphene via Raman spectroscopy at different excitation energies, Nano Lett. 11 (2011) 3190–3196.
[44] N.I. Kovtyukhova, P.J. Ollivier, B.R. Martin, T.E. Mallouk, S.A. Chizhik, E.V. Buzaneva, A.D. Gorchinskiy, Layer-by-Layer assembly of ultrathin composite films from micron-sized graphite oxide sheets and polycations, Chem. Mater. 11 (1999) 771–778.
[45] J. Li, M.L. Sham, J.-K. Kim, G. Marom, Morphology and properties of UV/ozone treated graphite nanoplatelet/epoxy nanocomposites, Compos. Sci. Technol. 67 (2007) 296–305.
[46] J. Li, L. Vaisman, G. Marom, J.-K. Kim, Br treated graphite nanoplatelets for improved electrical conductivity of polymer composites, Carbon 45 (2007) 744–750.
[47] L.M. Viculis, J.J. Mack, O.M. Mayer, H.T. Hahn, R.B. Kaner, Intercalation and exfoliation routes to graphite nanoplatelets, J. Mater. Chem. 15 (2005) 974–978.
[48] D. Cai, M. Song, Preparation of fully exfoliated graphite oxide nanoplatelets in organic solvents, J. Mater. Chem. 17 (2007) 3678–3680.